



OPEN

# $^{10}\text{Be}$ climate fingerprints during the Eemian in the NEEM ice core, Greenland

SUBJECT AREAS:

PALAEOCLIMATE  
CRYOSPHERIC SCIENCEAnna Sturevik-Storm<sup>1</sup>, Ala Aldahan<sup>1,2</sup>, Göran Possner<sup>3</sup>, Ann-Marie Berggren<sup>1</sup>, Raimund Muscheler<sup>4</sup>, Dorte Dahl-Jensen<sup>5</sup>, Bo M. Vinther<sup>5</sup> & Ilya Usoskin<sup>6</sup>Received  
9 September 2013Accepted  
19 August 2014Published  
30 September 2014Correspondence and  
requests for materials  
should be addressed to  
A.S.-S. (anna.sturevik\_  
storm@geo.uu.se)

<sup>1</sup>Uppsala University, Department of Earth Sciences, Villavägen 16 B, 752 36 Uppsala, Sweden, <sup>2</sup>Department of Geology, United Arab Emirates University, Al Ain, UAE, <sup>3</sup>Tandem Laboratory, Uppsala University, Lägerhyddsvägen 1, 751 20 Uppsala, Sweden, <sup>4</sup>Department of Geology, Lund University, Sölvegatan 12, 223 62 Lund, Sweden, <sup>5</sup>Centre for Ice and Climate, Niels Bohr Institute, University of Copenhagen, Juliane Maries Vej 30, 2100 Copenhagen K, Denmark, <sup>6</sup>Sodankylä Geophysical Observatory (Oulu unit) and Physics Dept., 90014 University of Oulu, Finland.

Several deep Greenland ice cores have been retrieved, however, capturing the Eemian period has been problematic due to stratigraphic disturbances in the ice. The new Greenland deep ice core from the NEEM site (77.45°N, 51.06°W, 2450 m.a.s.l) recovered a relatively complete Eemian record. Here we discuss the cosmogenic  $^{10}\text{Be}$  isotope record from this core. The results show Eemian average  $^{10}\text{Be}$  concentrations about 0.7 times lower than in the Holocene which suggests a warmer climate and approximately 65–90% higher precipitation in Northern Greenland compared to today. Effects of shorter solar variations on  $^{10}\text{Be}$  concentration are smoothed out due to coarse time resolution, but occurrence of a solar maximum at 115.26–115.36 kyr BP is proposed. Relatively high  $^{10}\text{Be}$  concentrations are found in the basal ice sections of the core which may originate from the glacial-interglacial transition and relate to a geomagnetic excursion about 200 kyr BP.

Drilling in North Greenland, through the North Greenland Eemian Ice Coring project (NEEM, 2007–2012), retrieved ice from the Eemian period (depth 2210–2430 m, 115.36–128.48 kyr BP<sup>1</sup>). Matching of several trace records from the NEEM core with the global  $\delta^{18}\text{O}_{\text{atm}}$  and  $\text{CH}_4$  in the NGRIP (North Greenland Ice core Project) and EDML (Epica Dronning Maud Land, Antarctica) cores<sup>2</sup> as well as variability in  $\text{N}_2\text{O}$ ,  $\delta^{15}\text{N}_{\text{atm}}$  and air content were used to establish the boundaries of the Eemian. Despite relatively good age estimation, missing climate transitions together with disturbances of the ice and obscured climate signals from ice below 2210 m hampered full interpretation of the stratigraphy. New  $^{10}\text{Be}$  isotope data presented here shed further light on these problems and provide in some part support to interpretations given by Dahl-Jensen et al.<sup>1</sup>, such as the warmer climate and the wet surface conditions during a part of the Eemian as well as the ice chronology.  $^{10}\text{Be}$  (half-life =  $1.387 \pm 0.012 \times 10^6$  years<sup>3</sup>;) is mainly produced in the atmosphere through spallation of oxygen and nitrogen by galactic cosmic rays (GCR) and their secondary particles, although there is a small production in the Earth's surface as well. The radionuclide is deposited on the Earth's surface through wet and/or dry fallout and is stored in natural archives such as ice and sediment. The production of  $^{10}\text{Be}$  is modulated by the variation in the strength of the geomagnetic field as well as by solar magnetic shielding. Changes in the local galactic surrounding may influence the cosmic ray flux but on much longer time scales. There are also several post-production and fallout processes (i.e. residence time in the atmosphere, scavenging rate, troposphere-stratosphere exchange, precipitation rate etc.) that can alter the final  $^{10}\text{Be}$  concentration found in the ice archive. There have been several attempts to model these processes and their interactions (for example<sup>4,5</sup>). One significant process is the dilution effect by precipitation, which commonly lowers  $^{10}\text{Be}$  concentration due to higher snow accumulation rate<sup>6–8</sup>. This dilution effect can be seen when comparing Greenland with Antarctic records or even within Antarctica at higher (i.e. closer to the coast) or lower precipitation rates regions (i.e. inland Antarctica<sup>9</sup>). Even though dry deposition always is present, it has greater impact in regions with very low precipitation, such as inner Antarctica, where the fraction of  $^{10}\text{Be}$  deposited by dry deposition is higher than that for wet deposition in such areas. This criterion of decreasing  $^{10}\text{Be}$  concentration with increasing precipitation, which can be related to changes in climate conditions, is established here through comparison of the Eemian climate conditions with the Holocene using the NEEM ice. Climatic conditions during the Eemian were expected to be 4–8°C warmer with a higher precipitation rate<sup>1</sup> than of the mean from last millennium. A possible cause of higher precipitation is missing Arctic sea ice



cover during the summer/autumn season allowing evaporation from the Arctic Ocean and thus increasing precipitation in northern Greenland resulting in a dilution of  $^{10}\text{Be}$  concentration.

## Results

Depth wise variability of  $^{10}\text{Be}$  concentration in the lowermost 320 m of the NEEM core (supplementary table S1) is shown in figure 1 where three apparent concentration parts are marked as A, B and C. The most shallow part, A, of the record (2201.65 m to 2307.25 m) indicates quite homogenous values with a low variance of 0.018 and a mean of  $1.15 \pm 0.06 \times 10^4$  atoms/ $\text{g}_{\text{ice}}$ . This part of the data does not show any clear trend but two peaks, at 2230 and 2279 m, occur and are significant within  $3\sigma$  standard deviation. These two peaks are associated with two weaker peaks at 2219 and 2302 m and will be discussed later in the text as  $P_1$  and  $P_2$  (figure 1).

Part B of the ice starts with the lowest  $^{10}\text{Be}$  concentrations found in the Eemian between 2307.25 and 2430.45 m depth (light blue-green shaded area, figure 1). A rising trend starts and continues until reaching a peak at 2428 m. Though the trend is clear, it is broken by two prominent dips at 2382 and 2402 m. Part C of the  $^{10}\text{Be}$  record, which most likely consists of ice older than the Eemian, follows after the peak at about 2428 and descends gradually to the lowest values of the whole sampled interval at around 2460 m which is followed by a peak at about 2475 m with the highest concentrations in this lowermost section of the NEEM core. A  $^{10}\text{Be}$  concentration of  $2.27 \times$

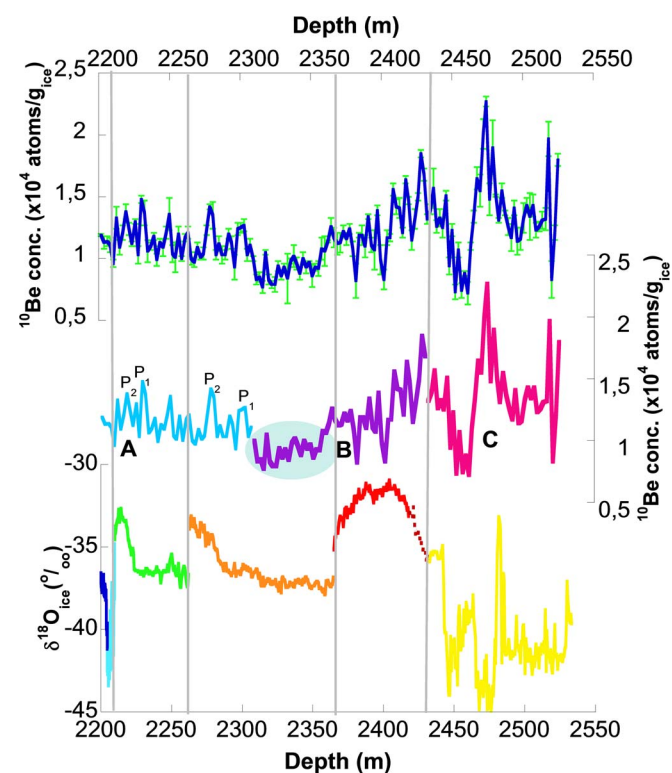


**Figure 1** |  $^{10}\text{Be}$  and  $\delta^{18}\text{O}_{\text{ice}}$  plotted depth-wise. The  $^{10}\text{Be}$  concentrations plotted as an undivided depth-series with error bars (blue line), in the apparent parts discussed in the text (blue = part A, purple = part B and pink = part C) and  $\delta^{18}\text{O}_{\text{ice}}$  plotted in the zones recognized by NEEM community members<sup>1</sup> (dark blue = zone 0, cyan = zone 1, green = zone 2, orange = zone 3, red = zone 4, dotted dark red = zone 5 and yellow = zone 6) depth wise for the lowermost 320 m of the NEEM deep ice core.  $P_1$  and  $P_2$  indicate the same peaks shown in figure 3 which are discussed in the text. Light blue-green shaded area shows the lowest  $^{10}\text{Be}$  concentrations found during the Eemian discussed in the text. The grey line shows where the ice is disturbed. Note that there are no disturbances between zone 4 and 5, hence both are different hues of red.

$10^4$  atoms/ $\text{g}_{\text{ice}}$  is measured for this peak; 3 times higher than the lowest value in the dip at around 2460 m. The last and deepest part of the core levels out until the last few samples which show a rapid fluctuation. The lowermost 3 samples (not shown in the graph) have very low concentrations of 0.41, 0.58 and  $0.53 \times 10^4$  atoms/ $\text{g}_{\text{ice}}$ .

In order to compare our measured Greenland Eemian  $^{10}\text{Be}$  concentrations and accumulation rates with the Holocene we have compiled available data from different Greenland ice cores in table 1. The mean Holocene  $^{10}\text{Be}$  concentrations range from  $0.72$  to  $1.79 \times 10^4$  atoms/ $\text{g}_{\text{ice}}$  and the mean Eemian  $^{10}\text{Be}$  concentration was measured to  $1.13 \times 10^4$  atoms/ $\text{g}_{\text{ice}}$ . It should however be noted that these ice cores do not cover the same periods of the Holocene nor the same geographical position; unfortunately there are not many overlapping long term Holocene  $^{10}\text{Be}$  records and we use the ones available today. The data, however, suggest higher concentrations at southern sites in Greenland.

We have illustrated the  $^{10}\text{Be}$  concentrations together with the accumulation rate in figure 2. Figure 2A shows all ice core  $^{10}\text{Be}$  concentrations and accumulation rates whilst figure 2B shows the same data but with the Renland and Milcent data removed as we are most interested in locations at the ice divide, more similar to the NEEM site. From the linear fits in figure 2A and 2B the mean Eemian  $^{10}\text{Be}$  concentration corresponds to an accumulation rate of  $\sim 0.42$  m/a and  $\sim 0.37$  m/a respectively. This accumulation rate is about 65–90% higher than of present-day NEEM accumulation rate of 0.22 m ice equivalent<sup>1</sup> (observe that the Holocene accumulation rate of 0.18 m given in table 1 is from early Holocene, not modern times).

## Discussion

The only Greenland ice core to be dated back into the Eemian is NGRIP and this record only extends to 123 BP. For this reason an Eemian chronology has been established by using the Antarctic EDML record, which reaches through the whole Eemian and has been linked to the NGRIP chronology. Hence, the EDML timescale has been used when converting the NEEM depth scale into chronology<sup>1</sup> (supplementary table S2), however it should be noted that the ice between 108–115 kyr BP is missing. This missing ice was attributed to ice movement associated with disturbance, folding and even faulting of the ice layers<sup>1</sup>.

The sampled Eemian interval was divided into seven different zones (0–6; figure 1) due to disturbance and folding in the ice as well as to different properties of the ice layers<sup>1</sup>. The first part of the core, earlier called part A, contains ice layers from 4 different zones (0–3) that are chronologically overlapping (figure 3). A few  $^{10}\text{Be}$  samples in the most upper part A of the ice belong to zones 0 and 1, but the majority of part A contains ice from zones 2 and 3. These later zones overlap a common time period due to folding of the ice and are well identified by the  $^{10}\text{Be}$  peaks and thus suggest repeated (faulted) ice layers. In particular, two peaks ( $P_1$  and  $P_2$ , figures 1 and 3, supplementary figure S1 and S2), of more or less the same concentration which also fits well with the  $\delta^{18}\text{O}$  concentrations, are found in zones 2 and 3. They relate to the same time period and are close to overlapping when plotted on the EDML timescale (arrows in figure 3). This can be seen as a confirmation that zones 2 and 3 have indeed been flipped and overlap one another. That the peaks are not exactly overlapping can be due to the coarse resolution in the  $^{10}\text{Be}$  record since the time span for each of the peaks represents an overlap for some hundred years (supplementary figure S2).

Part B comprises ice from zones 3–5 and the section of the ice with low  $^{10}\text{Be}$  concentration, between 2309.45 and 2353.45 m depth, is situated in the younger part of zone 3. Here the ice represents a very short time period, which has a higher resolution than the other parts of the Eemian ice. These low concentrations (figure 3) may result from (I) snow accumulation influences (i.e. increased precipitation) or (II) lower  $^{10}\text{Be}$  atmospheric production. Suggestion (I) would indicate a warmer climate with more precipitation which would be



**Table 1 | Mean  $^{10}\text{Be}$  concentration and accumulation rate in Greenland ice cores during periods of the Holocene; from North (Camp Century) to South (Dye 3). The time spans are given in BP (before present, i.e. before 1950). Observe that sites lying on the southern part of Greenland experience lower  $^{10}\text{Be}$  concentrations than sites further north. The mean concentrations consist of a different number of samples and are from different time spans within the Holocene period and from different geographical positions in Greenland. The table also show elevation and number of points used in the calculation for figure 2. The numbers of data, calculated points, are the ones for which both  $^{10}\text{Be}$  and accumulation rates were available, thus the temporal coverage vary from small series of a few samples to extensive ones covering hundreds of samples**

Ice core	Position	Mean $^{10}\text{Be}$ conc. ( $\times 10^4$ atoms/ $\text{g}_{\text{ice}}$ )	Concentration range of $^{10}\text{Be}$ ( $\times 10^4$ atoms/ $\text{g}_{\text{ice}}$ )	Mean accumulation rate (m/yr)	Elevation (m a.s.l)	Calculated points	Time period (BP)
Camp Century <sup>22,23</sup>	77°11' N 61°07' W	0.72	0.65–0.79	0.39	1885	2	7 869–164
NEEM	77°45' N 51°06' W	1.61*	0.77–2.46*	0.18	2450	59	11 195–9201
NGRIP <sup>24</sup>	75°10' N 42°32' W	1.79	0.76–3.88	0.19	2930	597	561–(45)**
Renland <sup>13</sup>	71°18' N 26°43' W	1.32	0.38–2.60	0.45	2340	57	19–(38)**
GISP 2 <sup>5</sup>	72°35' N 38°29' W	1.57	1.26–2.03	0.23	3203	27	3288–11647
GRIP <sup>7</sup>	72°58' N 37°64' W	1.50	1.11–1.96***	0.24	3246	317	About 305–9229
Milcent <sup>25</sup>	70°30' N 44°55' W	1.14	0.51–2.24	0.56	2410	116	769–148
Dye 3 <sup>26</sup>	65°11' N 43°50' W	1.06	0.35–2.14 (5.57)****	0.56	2480	573	526–(36)**
<b>All above Holocene Eemian (this work)</b>	77°45' N 51°06' W	<b>1.43</b> <b>1.13</b>	0.77–1.85	~0.37–~0.42		101	114 400–128 500

\*Unpublished data from the authors

\*\*Reaching in to more modern times gives BP (Before Present, i.e. 1950) negative values. (45), (38) and (36) BP is equal to AD 1995, 1988 and 1986 respectively.

\*\*\*Observe that the data is already smoothed with 11 m average  $^{10}\text{Be}$  concentration, actual range is greater.

\*\*\*\*Out of 573 samples, all spans between 0.35 and  $2.14 \times 10^4$  atoms/ $\text{g}_{\text{ice}}$ , one is with higher concentration of  $5.57 \times 10^4$  atoms/ $\text{g}_{\text{ice}}$ .

visible in a less negative  $\delta^{18}\text{O}_{\text{ice}}$  value, but instead the dip in  $^{10}\text{Be}$  concentration correlates with a dip in the  $\delta^{18}\text{O}_{\text{ice}}$  value indicating colder climate. If suggestion (II) is correct, we would observe an increase in the geomagnetic field (figure 4) or an increase in solar activity, though independent high resolution data for the Eemian for these two variables are not available. This leaves us with two alternatives, either the low  $^{10}\text{Be}$  concentration is due to a period with lower temperatures and higher precipitation which could be seen as an unusual climatic signal or it might be due to a period of high geomagnetic strength or increased solar activity. The Sun has spent approximately three quarters of its time in a moderate activity during the Holocene<sup>10</sup>. The rest of the Holocene solar activity can be divided between grand maxima and grand minima. There are two different types of grand minima, the shorter Maunder-like ones 30–90 years in duration and the longer, Spörer-like >110 years in duration. These grand maxima and minima do not occur in a cyclic manner, but form stochastic/chaotic processes, even though this is debated. Considering similar solar activity fluctuations during the Eemian would mean that about a quarter of time the  $^{10}\text{Be}$  concentration found in the NEEM core could have been higher or lower due to changes in solar activity. However, the coarse resolution of the  $^{10}\text{Be}$  record, with an average of 140 years during the Eemian, makes it impossible to capture short grand minima. The range of  $^{10}\text{Be}$  production rate varies, due to solar activity, within  $\pm 30\%$ <sup>11</sup>, which is too small to explain any of the observed large changes in  $^{10}\text{Be}$  concentration. With the present resolution, grand minima and maxima of solar activity are smoothed out and thus leading to a barely observable effect of about 10%. Changes in the geomagnetic field may be more relevant for large changes in the  $^{10}\text{Be}$  concentration, e.g., a geomagnetic excursion with the dipole moment being reduced to 10% that would lead to a factor of 2–3 enhancements (peaks) of the global  $^{10}\text{Be}$  production<sup>11</sup>. Duration of such rare events is hundreds-thousands of years and a short-term dip in  $^{10}\text{Be}$  cannot be even hypothetically attributed to the geomagnetic field change since it takes much longer time to intensify the field intensity.

The first part of zone 4 covers a period that also is overlapped by ice from zone 2 and 3, i.e. one time period is represented by 3 sections in the ice core. Otherwise there are no major changes in the appearance of zone 4 and zone 5 chronologically. In zone 4, the major dips in  $^{10}\text{Be}$  concentrations are anti-correlated with the peaks in  $\text{CH}_4$  which indicate melting of ice layers. If we exclude production variations to be the cause of this relationship, the likely explanation is reduced  $^{10}\text{Be}$  concentration caused by a higher precipitation rate in the warmer climate as indicated by the melt layers. Zone 4 has a mean  $^{10}\text{Be}$  value of  $1.20 \times 10^4$  atoms/ $\text{g}_{\text{ice}}$  with a standard deviation of  $0.19 \times 10^4$  atoms/ $\text{g}_{\text{ice}}$ , leaving two dips as statistically significant in zone 4, both with concentrations close to  $0.8 \times 10^4$  atoms/ $\text{g}_{\text{ice}}$ . Significant peaks appear only in the lower part of zone 4 situated closest to zone 5. These peaks could be interpreted as part of a decreasing trend from a drier and probably colder period with higher  $^{10}\text{Be}$  concentrations toward the much warmer and possibly wetter Eemian period with lower  $^{10}\text{Be}$  concentrations. The interpretation as a declining trend from an earlier colder period also appears plausible when looking at zone 5 and the  $\delta^{18}\text{O}$  record, which supports the hypothesis that the dips in  $^{10}\text{Be}$  concentration in zone 4 are caused by a higher precipitation rate due to warmer climate spells. When the different zones shown in figure 1 are put on the EDML time scale (figure 3) and compared with the  $\delta^{18}\text{O}_{\text{ice}}$  and air content, there appears to be a rising tendency in these records from the beginning of the Eemian at about 128 kyr BP to about 125 kyr BP, but the tendencies slowly decline at about 120 kyr BP until the end of the Eemian record at about 115 kyr BP.  $^{10}\text{Be}$  concentration, on the other hand, shows a declining tendency during the early Eemian (figure 4).

The deepest part of the core, (part C or zone 6) containing the lowermost 100 m of ice and is left undated and hence only represented in figure 1, starts with the most prominent dip encountered in

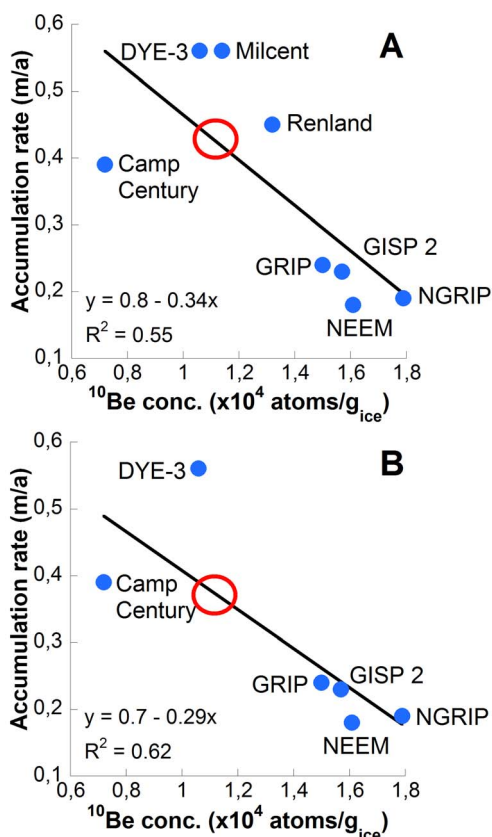


**Figure 2** | Accumulation rate plotted against mean  $^{10}\text{Be}$  concentrations for different periods during the Holocene. The listed accumulation rates cover the corresponding period of the  $^{10}\text{Be}$  concentrations within the Holocene for each measurement point, however the spanned time period can differ between the different sites. It should be noted that different standards have been used for some of the samples when calculating the concentrations, as well as different measuring procedures (filtering, no filtering of the samples etc.), which can result in an error of  $\pm 10\%$  between the different cores. The red ring shows the mean Eemian  $^{10}\text{Be}$  concentration of  $1.13 \times 10^4$  atoms/g<sub>ice</sub> on the correlation line and indicates annual precipitation of around 0.35 to just above 0.4 m ice equivalent at NEEM during the Eemian. It should be noted that Milcent and Renland, plot A, are situated far from the ice divide why they are removed from plot B where only sites at or close to the ice divide are included.

the 320 m long  $^{10}\text{Be}$  record. This dip correlates with less negative  $\delta^{18}\text{O}_{\text{ice}}$  and could hence also be interpreted as a warm period with more precipitation. Even though the period seems to be warmer, it does not reach interglacial temperatures as indicated by  $\delta^{18}\text{O}_{\text{ice}}$ , even though the  $^{10}\text{Be}$  values reach the lowest concentration in the core. We conjecture this could be due to a slightly warmer precipitation-rich period within the glacial period or to a period with very low  $^{10}\text{Be}$  production rates. The broad  $^{10}\text{Be}$  peak at about 2475 m depth has the highest concentration from the bottom part of the ice core with levels as high as during glacial time. This peak is not anti-correlated with  $\delta^{18}\text{O}_{\text{ice}}$ , though the oxygen isotopes values are low, as is often seen during a glacial period, but suggesting an influence of changes in the activity either of the Sun or of the Earth's magnetic field. Since there is evidence in the  $^{10}\text{Be}$  record for association of high concentration during excursions in the Earth's magnetic field<sup>12–15</sup>, we hypothesize that the peak might be due to a magnetic excursion such as the Iceland basin (IB) excursion around 180–190 kyr BP<sup>16,17</sup> or the Jamaica/Pringle fall at 205–215 kyr BP<sup>17,18</sup>. Assuming this ice to be around 200 kyr old, about 10% of the original  $^{10}\text{Be}$  concentration

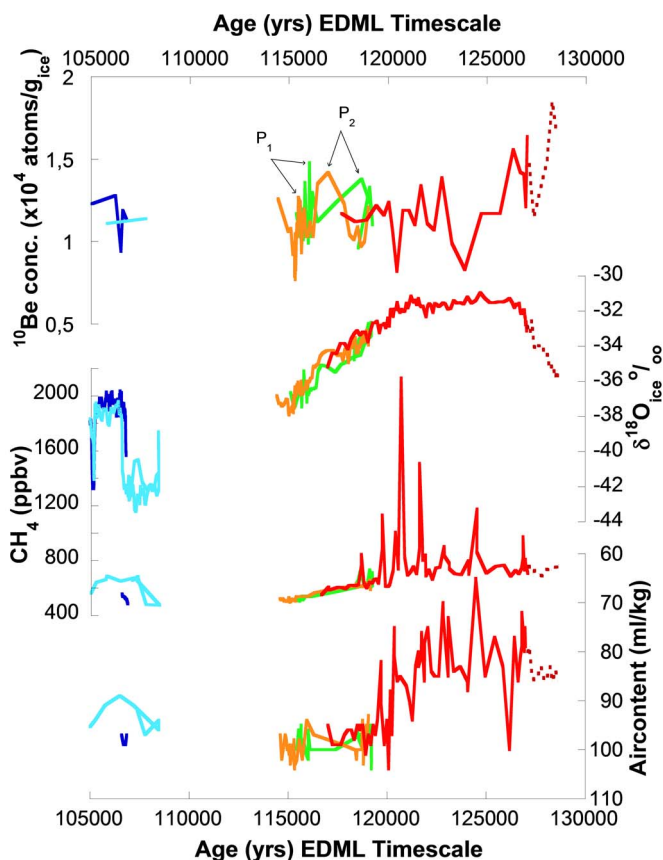


**Figure 3** |  $^{10}\text{Be}$  concentrations  $\delta^{18}\text{O}$ ,  $\text{CH}_4$  and air content on the EDML time scale.  $^{10}\text{Be}$  concentrations put on the EDML time scale with  $\delta^{18}\text{O}$ ,  $\text{CH}_4$  and air content showing the dips in  $^{10}\text{Be}$  concentration and correlation with peaks in  $\text{CH}_4$  as well as low air content. The black arrows marked P<sub>1</sub> and P<sub>2</sub> indicate peaks that could be correlated to each other in the different zones. The zones are color coded as follows, zone 0 is blue, zone 1 cyan, zone 2 green, zone 3 orange, zone 4 red and zone 5 dark red. Observe that zone 2 and 3 are reversed and overlapping when put in chronological order.

would have decayed which would put the original concentration at approximately  $2.5 \times 10^4$  atoms/g<sub>ice</sub>. If the  $^{10}\text{Be}$  peak is from an excursion around 200 kyr, the narrow peak in  $\delta^{18}\text{O}$  at 2480 m depth could be derived from the interglacial before the Eemian which occurred close to 200 kyr, clearly visible in the Vostok core for example<sup>19</sup>. The  $^{10}\text{Be}$  concentration in the ice below this peak more or less levels out to values comparable to warmer periods even though the  $\delta^{18}\text{O}$  indicates colder periods. The last few meters of measured  $^{10}\text{Be}$  in the NEEM ice core show high variability which may relate to mixing with bottom sediments since it is known that  $^{10}\text{Be}$  easily gets attached to sediments and hence ice layers with high sediment content can be enriched in  $^{10}\text{Be}$ .

Even though the Blake geomagnetic excursion has proven hard to date, it has been placed between 110 and 125 kyr BP<sup>17,18</sup>. In the NEEM core, there is no sign of any excursions around this interval in the  $^{10}\text{Be}$  record. However, a big section of ice spanning 108–115 kyr BP on the EDML time scale is, as earlier discussed, missing. If the duration of the Blake event is less than 7 kyr, it is likely that it could have appeared in the time period where the ice is missing i.e. between 108 and 115 kyr BP.

Eemian  $^{10}\text{Be}$  concentrations are on average about 0.7 times lower than in the Holocene samples measured from the NEEM core. This lower concentration could be interpreted as the Eemian climate in Northern Greenland experienced about 65–90% higher precipitation

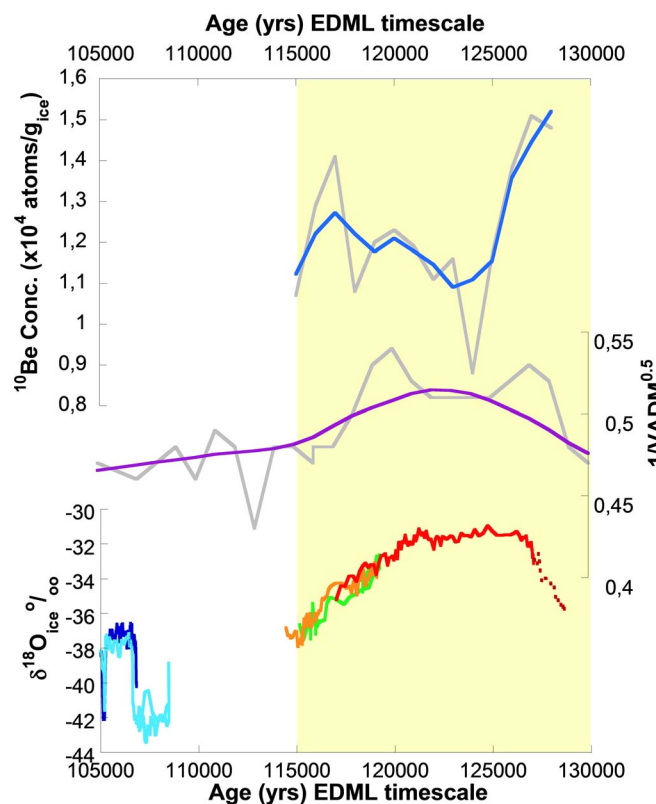


**Figure 4** |  $^{10}\text{Be}$  concentrations, Virtual Axis Dipole Moment and  $\delta^{18}\text{O}_{\text{ice}}$  on the EDML time scale.  $^{10}\text{Be}$  concentrations interpolated on a time scale with a resolution of 1000 years (upper grey line) weighted with 36% (light blue) plotted with  $1/\text{VADM}^{0.5}$  (lower grey line)<sup>20</sup> weighted with 15% (purple) and  $\delta^{18}\text{O}_{\text{ice}}$  (rainbow). The yellow shade background indicates the Eemian period.

rate than it does today provided the inverse relationship between precipitation and  $^{10}\text{Be}$  concentrations persisted through time. Most solar grand minima and maxima are smoothed out due to the coarse resolution. There is, however, a part of the  $^{10}\text{Be}$  record between 115.26 and 115.36 kyr BP which has a higher time resolution of just some decades and shows a persistent low  $^{10}\text{Be}$  concentration. This feature may relate to a solar maximum. The high  $^{10}\text{Be}$  concentrations in the lower section of the Eemian layers most likely originate from the glacial-interglacial transition rather than decreased solar activity. The highest  $^{10}\text{Be}$  concentration in this section of ice may relate to a magnetic excursion at about 200 kyr BP.

## Methods

Samples used here are ice core sawdust gathered from when the ice core was divided along the length. Each of the 151 samples consisted of ice sawdust from 2.2 m core and the weight of the samples lay between 233 and 444 g. This gave the samples an average age of 140 years per sample during the Eemian. As each ice sawdust sample is homogeneously mixed within the sample bag there is no possibility to divide the samples with regard to smaller intervals. The collection equipment was thoroughly cleaned between each sampling event using a brush to reduce cross contamination as much as possible. The use of ice sawdust for  $^{10}\text{Be}$  analysis is a new approach which to our knowledge has never been tested before; it minimizes the waste of valuable ice core material and opens the possibility for obtaining continuous  $^{10}\text{Be}$  record. Since this ice is from the lowermost part of the core, the samples, unavoidably, contain traces of drilling fluid consisting of Estisol 240 and Coasol which is not expected to contain any  $^{10}\text{Be}$ . Before melting the ice sample, 100 microgram of  $^9\text{Be}$ -carrier (Scharlau product 00S007 having  $^{10}\text{Be}/^9\text{Be}$  value of  $10^{-15}$ ) was added. The water was, without filtration, loaded into disposable ion exchange columns into (Bio-Rad Poly-Prep Prefilled Chromatography Columns AG 50 W-X8 resin 100–200 mesh hydrogen form  $0.8 \times 4$  cm). No visible dust grains were noticed in the samples before being loaded into the columns. The  $^{10}\text{Be}$  and  $^9\text{Be}$  were extracted from the column using 4 M HCl and Be-hydroxide was precipitated using  $\text{NH}_3$  and then left overnight. The beryllium-hydroxide reduced to BeO by heating to a temperature of  $600^\circ\text{C}$  at a final

yield of  $>85\%$ . Nb-powder was mixed with the BeO and the mixture was pressed into target for accelerator mass spectrometry (AMS) measurements. The Uppsala University AMS system was used for the measurement at a terminal voltage of 4.7 MV using 40 sample MC-SNICS (NEC) ion source and ion-beam current at  $0.5\text{--}1 \mu\text{A}^{21}$ . Each sample was measured for three cycles for up to 20 minutes per sample. Isobaric interference from  $^{10}\text{B}$  was additionally reduced one order of magnitude through use of a second stripper foil and a vertical  $180^\circ$  dipole magnet installed before the detector system. The concentration of  $^{10}\text{Be}$  were calculated using the NIST SRM 4325 standard ( $^{10}\text{Be}/^9\text{Be} = 3.03 \times 10^{-11}$ , internally standardized value) at machine and statistical errors  $<15\%$ . Although the mean average error of the samples is around 5.6%, the variability from one sample to another is related to variability in counting rates that is affected by sample current and amount of Nb-BeO mixture remaining in the cathode. Blanks were prepared following the same sample procedure and the blank values were  $\geq 3 \times 10^{-15}$ , which is two magnitudes smaller than the ice sample average of  $3 \times 10^{-13}$ .

- Dahl-Jensen, D. *et al.* Eemian interglacial reconstructed from a Greenland folded ice core. *Nature* **493**, 489–494 (2013).
- Capron, E. *et al.* Synchronising EDML and NorthGRIP ice cores using delta O-18 (atm) and CH4 measurements over MIS5 (80–123 kyr). *Quaternary Sci. Rev.* **29**, 222–234; DOI:10.1016/j.quascirev.2009.07.014 (2010).
- Korschinek, G. *et al.* A new value for the half-life of  $^{10}\text{Be}$  by Heavy-Ion Elastic Recoil Detection and liquid scintillation counting. *Nucl. Instrum. Meth. B* **268**, 187–191 (2010).
- Field, C. V., Schmidt, G. A., Koch, D. & Salyk, C. Modeling production and climate-related impacts on  $^{10}\text{Be}$  concentration in ice cores. *J. Geophys. Res.-Atmos.* **111**, D15107; DOI:10.1029/2005jd006410 (2006).
- Heikkilä, U. & Smith, A. Production rate and climate influences on the variability of  $^{10}\text{Be}$  deposition simulated by ECHAM5-HAM globally, in Greenland and in Antarctica. *J. Geophys. Res.-Atmos.* **118**, 2506–2520 (2013).
- Raisbeck, G. M. *et al.* Cosmogenic  $^{10}\text{Be}$  concentrations in Antarctic ice during the past 30,000 years. *Nature* **292**, 825–826; DOI:10.1038/292825a0 (1981).
- Yiou, F. *et al.* Beryllium 10 in the Greenland Ice Core Project ice core at Summit, Greenland. *J. Geophys. Res.-Oceans* **102**, 26783–26794; DOI:10.1029/97jc01265 (1997).
- Finkel, R. C. & Nishiizumi, K. Beryllium 10 concentrations in the Greenland Ice Sheet Project 2 ice core from 3–40 ka. *J. Geophys. Res.-Oceans* **102**, 26699–26706; DOI:10.1029/97jc01282 (1997).
- Berggren, A. M. *et al.* Variability of  $^{10}\text{Be}$  and  $\delta^{18}\text{O}$  in snow pits from Greenland and a surface traverse from Antarctica. *Nucl. Instrum. Meth. B* **294**, 568–572 (2013).
- Usoskin, I. G., Solanki, S. K. & Kovaltsov, G. A. Grand minima and maxima of solar activity: new observational constraints. *Astron. Astrophys.* **471**, 301–309; DOI:10.1051/0004-6361/20077704 (2007).
- Kovaltsov, G. A. & Usoskin, I. G. A new 3D numerical model of cosmogenic nuclide Be-10 production in the atmosphere. *Earth. Planet. Sc. Lett.* **291**, 182–188; DOI:10.1016/j.epsl.2010.01.011 (2010).
- Raisbeck, G. M. *et al.* Evidence for two intervals of enhanced  $^{10}\text{Be}$  deposition in Antarctic ice during the last glacial period. *Nature* **326**, 273–277; DOI:10.1038/326273a0 (1987).
- Aldahan, A. *et al.* Sixty year  $^{10}\text{Be}$  record from Greenland and Antarctica. *P. Indian AS -Earth* **107**, 139–147 (1998).
- Aldahan, A. & Possnert, G. Geomagnetic and climatic variability reflected by  $^{10}\text{Be}$  during the Quaternary and late Pliocene. *Geophys. Res. Lett.* **30**, DOI:10.1029/2002gl016077 (2003).
- Aldahan, A., Possnert, G., Peck, J., King, J. & Colman, S. Linking the  $^{10}\text{Be}$  continental record of Lake Baikal to marine and ice archives of the last 50 ka: Implication for the global dust-aerosol input. *Geophys. Res. Lett.* **26**, 2885–2888; DOI:10.1029/1999gl900469 (1999).
- Knudsen, M. F., Henderson, G. M., Frank, M., Mac Niocaill, C. & Kubik, P. W. In-phase anomalies in Beryllium-10 production and palaeomagnetic field behaviour during the Iceland Basin geomagnetic excursion. *Earth. Planet. Sc. Lett.* **265**, 588–599; DOI:10.1016/j.epsl.2007.10.051 (2008).
- Channell, J. E. T. Late Brunhes polarity excursions (Mono Lake, Laschamp, Iceland Basin and Pringle Falls) recorded at ODP Site 919 (Irminger Basin). *Earth. Planet. Sc. Lett.* **244**, 378–393; DOI:10.1016/j.epsl.2006.01.021 (2006).
- Langereis, C. G., Dekkers, M. J., deLange, G. J., Paterne, M. & vanSantvoort, P. J. M. Magnetostratigraphy and astronomical calibration of the last 1.1 Myr from an eastern Mediterranean piston core and dating of short events in the Brunhes. *Geophys. J. Int.* **129**, 75–94; DOI:10.1111/j.1365-246X.1997.tb00938.x (1997).
- Petit, J. R. *et al.* Climate and atmospheric history of the past 420,000 years from the Vostok ice core, Antarctica. *Nature* **399**, 429–436; DOI:10.1038/20859 (1999).
- Guyodo, Y. & Valet, J.-P. Global changes in the intensity of the Earth's magnetic field during the past 800 kyr. *Nature* **399**, 249–252 (1999).
- Berggren, A.-M., Possnert, G. & Aldahan, A. Enhanced beam currents with coprecipitated niobium as a matrix for AMS measurements of  $^{10}\text{Be}$ . *Nucl. Instrum. Meth. B* **268**, 795–798; DOI:10.1016/j.nimb.2009.10.033 (2010).
- Beer, J. *et al.* The Camp Century  $^{10}\text{Be}$  record: implications for long-term variations of the geomagnetic dipole moment. *Nucl. Instrum. Meth. B* **5**, 380–384; DOI:10.1016/0168-583x(84)90545-7 (1984).



23. Beer, J. *et al.* Information on past solar activity and geomagnetism from  $^{10}\text{Be}$  in the Camp Century ice core. *Nature* **331**, 675–679; DOI:10.1038/331675a0 (1988).
24. Berggren, A. M. *et al.* A 600-year annual  $^{10}\text{Be}$  record from the NGRIP ice core, Greenland. *Geophys. Res. Lett.* **36**; DOI:10.1029/2009gl038004 (2009).
25. Beer, J. *et al.* Temporal  $^{10}\text{Be}$  variations. *18th Int. Cosmic Ray Conf. Conf. Papers* **319**, 317–320 (1983).
26. Beer, J. *et al.* Temporal  $^{10}\text{Be}$  variations in ice. *Radiocarbon* **25**, 269–278 (1983).

## Acknowledgments

We acknowledge financial support from the Swedish Research Council. NEEM is directed and organized by the Center of Ice and Climate at the Niels Bohr Institute and US NSF, Office of Polar Programs. It is supported by funding agencies and institutions in Belgium (FNRS-CFB and FWO), Canada (NRCan/GSC), China (CAS), Denmark (FIST), France (IPEV, CNRS/INSU, CEA and ANR), Germany (AWI), Iceland (RannIs), Japan (NIPR), Korea (KOPRI), The Netherlands (NWO/ALW), Sweden (VR), Switzerland (SNF), United Kingdom (NERC) and the USA (US NSF, Office of Polar Programs). I.U. acknowledges the financial support by the Academy of Finland to the ReSoLVE Center of Excellence (project no. 272157).

## Author contributions

A.S.-S. contributed to collection (in Greenland) and chemical preparation of samples and together with A.A., G.P. and A.-M. B. designed the investigation, performed data analyses and interpretation and prepared the first draft of the paper. G.P. ran the AMS measurements. R.M., D.D.-J. and B.M.V. contributed to the drilling in Greenland and data interpretation. I.U. contributed to the interpretations regarding the solar variations. All authors were involved in the discussion and writing of the final manuscript.

## Additional information

Supplementary information accompanies this paper at <http://www.nature.com/scientificreports>

**Competing financial interests:** The authors declare no competing financial interests.

**How to cite this article:** Sturevik-Storm, A. *et al.*  $^{10}\text{Be}$  climate fingerprints during the Eemian in the NEEM ice core, Greenland. *Sci. Rep.* **4**, 6408; DOI:10.1038/srep06408 (2014).



This work is licensed under a Creative Commons Attribution-NonCommercial-ShareAlike 4.0 International License. The images or other third party material in this article are included in the article's Creative Commons license, unless indicated otherwise in the credit line; if the material is not included under the Creative Commons license, users will need to obtain permission from the license holder in order to reproduce the material. To view a copy of this license, visit <http://creativecommons.org/licenses/by-nc-sa/4.0/>